



OPEN ACCESS

EDITED BY

Nalan Kabay,
Ege University, Türkiye

REVIEWED BY

Zhongyun Liu,
Georgia Institute of Technology, United States
Aydın Cihanoğlu,
Ege University, Türkiye
Enver Güler,
Atılım University, Türkiye

*CORRESPONDENCE

Anna Siekierka,
✉ anna.siekierka@pwr.edu.pl

RECEIVED 23 February 2024

ACCEPTED 08 April 2024

PUBLISHED 02 May 2024

CITATION

Muratow M, Yalcinkaya F, Bryjak M and Siekierka A (2024), Surface-modified PVDF membranes for separation of dye by forward osmosis.
Front. Membr. Sci. Technol. 3:1390727.
doi: 10.3389/frmst.2024.1390727

COPYRIGHT

© 2024 Muratow, Yalcinkaya, Bryjak and Siekierka. This is an open-access article distributed under the terms of the [Creative Commons Attribution License \(CC BY\)](https://creativecommons.org/licenses/by/4.0/). The use, distribution or reproduction in other forums is permitted, provided the original author(s) and the copyright owner(s) are credited and that the original publication in this journal is cited, in accordance with accepted academic practice. No use, distribution or reproduction is permitted which does not comply with these terms.

Surface-modified PVDF membranes for separation of dye by forward osmosis

Marta Muratow¹, Fatma Yalcinkaya², Marek Bryjak¹ and Anna Siekierka^{1*}

¹Wrocław University of Science and Technology, Faculty of Chemistry, Wrocław, Poland, ²Technical University of Liberec, Faculty of Mechatronics, Liberec, Czechia

Modification of membranes is widely used for altering their separation properties. In this study, the modification of PVDF nanofiber mat by deposition of polyamide layers was evaluated to improve dye recovery by means of forward osmosis process. The polyamide active layer was prepared by a reaction of cyclic aromatic amines, *m*-phenylenediamine, or piperazine, and trimesoylchloride. The modification progress was monitored by FTIR analysis, water uptake, nitrogen content, and grafting yields. Investigated membranes showed an excellent dye separation features with water flux and dye fluxes strongly related to type of applied amines and reaction time. The best obtained membrane demonstrated outstanding performance in forward osmosis; their water flux was 3.3 LMH and rejection rate of 97% for bromocresol green dye. The membrane allowed increase dye concentration by 50% after 24 h of the process.

KEYWORDS

PVDF, dye concentration, forward osmosis, piperazine, phenylenediamine

1 Introduction

Wastewaters from industrial sources, containing a combination of organic compounds and salts, pose ongoing challenges in meeting goals for minimal or zero liquid discharge, as well as resource recovery (Li et al., 2023). Treating such wastewater streams is significantly challenged by elevated content of organic compound, which can hinder the effectiveness of traditional methods like advanced oxidation processes, biological treatments, carbon adsorption, membrane separation, and UV ozonation (Lin et al., 2020). Among the mentioned methods, membrane separation is extensively utilized due to its straightforward operation, minimal chemical requirements, and comprehensive removal of pollutants across varying sizes. Nevertheless, the traditional pressure-driven membrane separation techniques rely on hydraulic pressure application, leading to drawbacks such as heightened fouling susceptibility, increased cleaning frequency, and shortened membrane lifespan. Hence, there is a critical need for the development of innovative membrane technologies to address these challenges (Zhao et al., 2015).

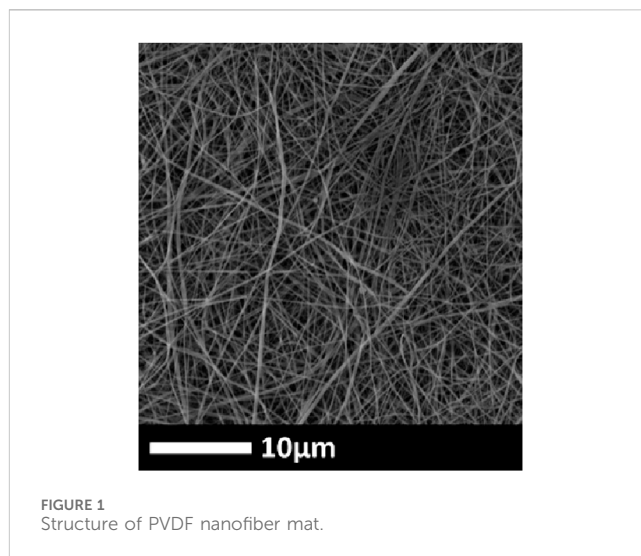
Forward osmosis (FO), a membrane process driven by osmotic forces, has emerged as a viable alternative for water and wastewater treatment. FO, unlike reverse osmosis, offers numerous potential advantages, including reduction of operating pressure and a decreasing of fouling phenomenon (Peng et al., 2020). Presently, thin film composite (TFC) polyamide membranes are widely utilized in forward osmosis applications (Fam et al., 2014; Huang and McCutcheon, 2015; Alihemati et al., 2020). Existing literature predominantly highlights their critical attribute of high salt rejection, particularly concerning NaCl. However, this

high salt rejection often accompanies reduced water permeability due to an inherent tradeoff. Moreover, the retention of salts from the feed solution can lead to their accumulation, thereby diminishing the osmotic driving force and subsequently lowering the FO water flux (Peng et al., 2020). While salt rejection remains a crucial parameter for desalination-focused applications, its significance may not be as pronounced for forward osmosis processes employed for non-desalination purposes. As an example, in the pretreatment stage of seawater desalination with forward osmosis, the primary objective should be the removal of algae and scalants (such as calcium and magnesium sulfates) to mitigate the potential risks of biofouling and scaling in the subsequent reverse osmosis process (Achilli et al., 2009). In an osmotically-driven membrane bioreactor, a high level of salt rejection could paradoxically diminish bioactivity, which is undesirable for the process. (Achilli et al., 2009; Xiao et al., 2011; Qiu and Ting, 2013). It is presumed that an ideal forward osmosis membrane should be tailored and fine-tuned to suit specific applications, allowing for the selective retention or recovery of valuable compounds.

Recent research has directed attention towards various polymer materials utilized in the fabrication of forward osmosis membranes. These materials include cellulose derivatives, polyamide, various polyelectrolyte, and polybenzimidazole (Alihemati et al., 2020). Cellulose derivatives like cellulose triacetate membranes are produced as flat sheets and hollow fibers using the phase inversion process followed by heat treatment. Nonetheless, the traditional thin film composite reverse osmosis membrane, featuring a hydrophobic phase-inversion polysulfone supporting layer and a thick nonwoven fabric backing layer, has consistently underperformed in forward osmosis trials due to significant mass transfer resistance near the interface of the selective thin film layer (Huang et al., 2016).

Electrospun nanofibers represent a category of material characterized by inherently high porosity and an interconnected pore structure (Yalcinkaya et al., 2017; Torres-Mendieta et al., 2020; Havelka et al., 2023). These distinctive attributes render nanofiber mats highly favorable as potential support materials for thin film composite forward osmosis (TFC-FO) membranes. A membrane material intended for forward osmosis applications should possess hydrophilic properties along with robust thermal and chemical resistance, as well as exceptional mechanical strength. The utilization of PVDF in the fabrication of TFC-FO membranes is advocated due to its outstanding thermal, mechanical, and chemical characteristics (Ndiaye et al., 2022).

In this study, the polyamide thin film composite PVDF membranes, received by reactions of TMC and MPDA, or TMC and PIP, were explored. The chemical and physical analyses of prepared membranes were done. They included the functional groups' analysis, water content, nitrogen content, or grafting yields. Systematic investigations of FO separation performance including water permeability, dye rejection, and dye concentration were performed. The



outcomes of the studies broaden the scope of applications for forward osmosis-based separation processes, particularly before desalination. They might stimulate the development of innovative membranes capable for highly selective rejection of target solutes tailored for some specific applications.

2 Materials and methods

2.1 Materials

Hexane, 97%, piperazine (PIP), 99%, 1,3,5-Benzenetricarbonyl chloride (Trimesoylchloride-TMC), 97%, m-phenylenediamine (MPDA) were delivered by Sigma- Aldrich. D-(+)- glucose and bromocresol green were delivered by POCH, Poland.

2.2 PVDF nanofibers preparation

The nanofibers were prepared through direct current (+55 kV, -15 kV) electrospinning of PVDF (13 wt%, Solef 1015) dissolved in N, N-dimethylformamide (DMF, Penta s. r.o.). The electrospinning process was performed using an electrospinning system (Nanospider, NS 8S1600U, Elmarco), and the produced nanofibers were collected over silicone paper. Secondly, the fibers were laminated over a spun-bond polyethylene terephthalate (PET) nonwoven fabric (100 g m⁻²) previously coated with a 12 g m⁻² co-polyamide adhesive web (Protechnic, Cernay, France). Finally, a heat press (HLV 150, Pracovní stroje Teplice s. r.o.) was employed to promote the lamination process at 130°C and 50 kN for 3 min, resulting in a proper union between the nanofiber net and the support. The SEM image of pristine PVDF is shown in Figure 1.

TABLE 1 Nitrogen content for investigated membranes.

Sample	PVDF	PVDF-PDA-1min	PVDF- PDA-2 min	PVDF-PIP-1 min	PVDF-PIP-2 min
Z _n [mmol/g]	0	0.13	0.25	0.19	0.22

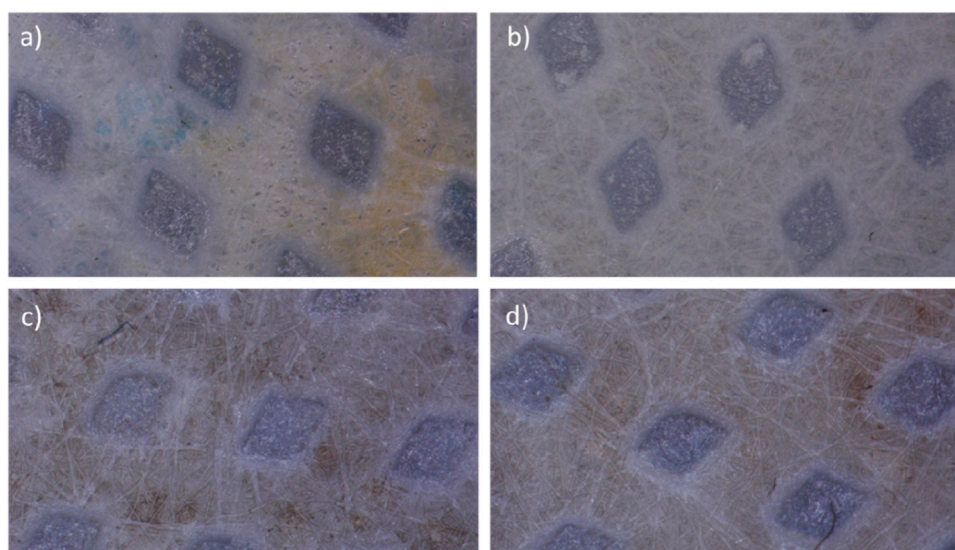


FIGURE 2
Modified membranes PVDF by PDA by (A) 1 min and (B) 2 min, by piperazine by (C) 1 min and (D) 2 min (x40 magnification).

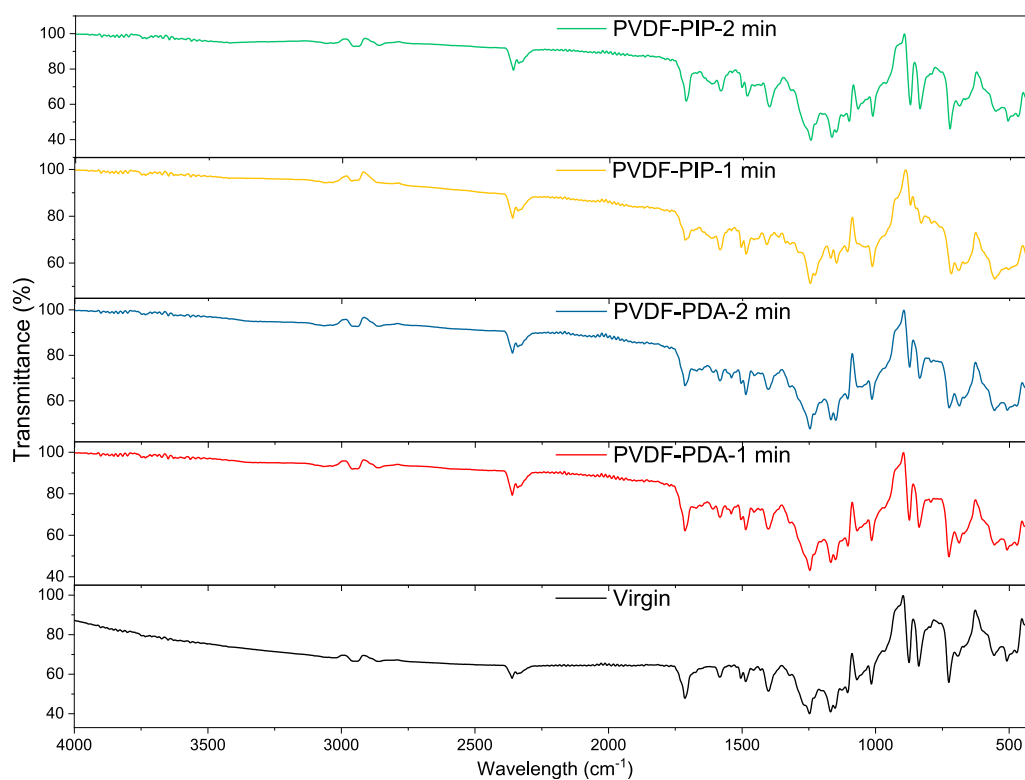


FIGURE 3
FTIR spectra from investigated membranes.

The previous findings demonstrated that laminated composite PVDF nanofiber membranes had a notable tensile strength of 133 N/5 cm in the machine direction and 107 N/5 cm in the counter direction (Islam et al., 2022). Moreover,

the membranes demonstrated enhanced chemical resistance when subjected to extreme acidic and basic conditions, as well as a range of chemical agents (Gul et al., 2022; Havelka et al., 2023).

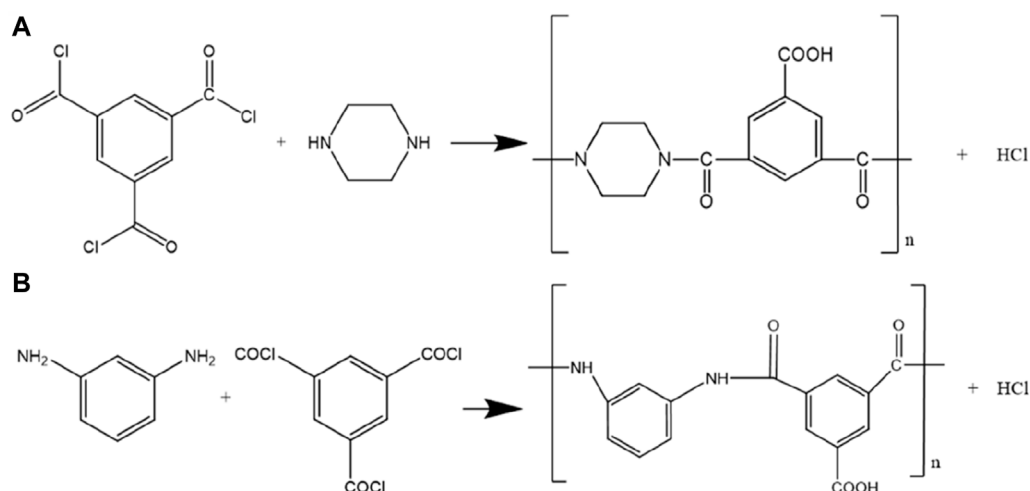


FIGURE 4
Reactions between TMC and (A) PIP, (B) MPDA.

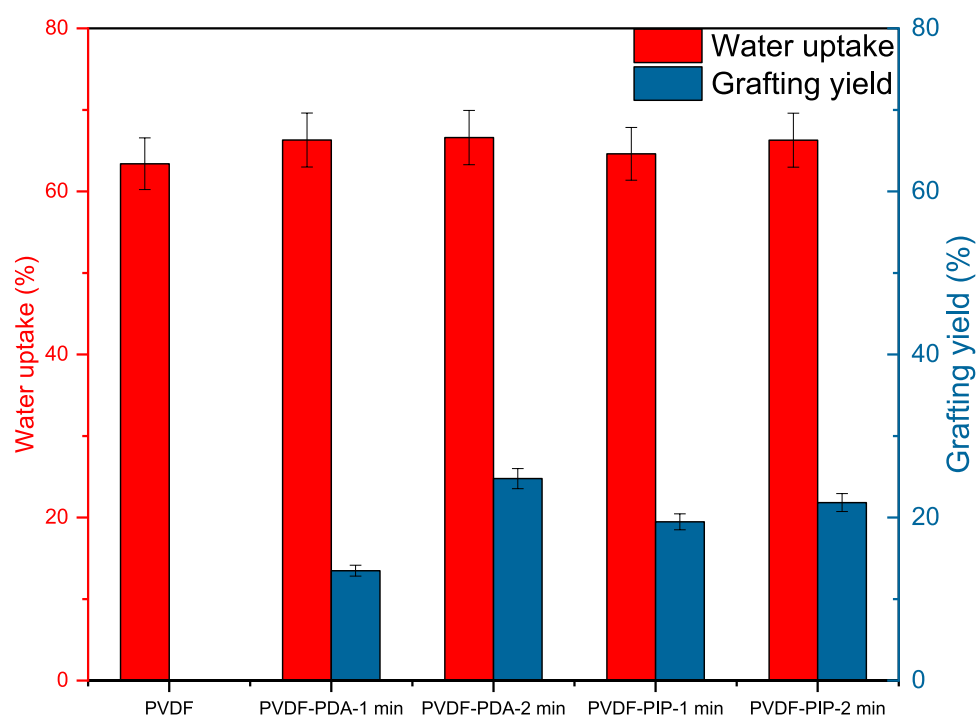


FIGURE 5
Water uptake and grafting yield of the investigated membranes.

2.3 FO membrane preparation

Laminated PVDF nanofibers were modified separately by PIP and MPDA. Firstly, The PVDF nanofibers were immersed in 4 wt% PIP or MPDA for 2 min. Then the soaked membranes were immersed in TMC (0.5% wt. in hexene) for 1 or 2 min. In the next step, membranes were put to an oven kept there for 8 min at 80°C. After that, four different membranes were obtained. They were encoded as PVDF-PIP-1, PVDF-PIP-2,

PVDF-MPDA-1, and PVDF-MPDA-2. Here, PIP-1, PIP-2, MPDA-1, and MPDA-2 describe used diamine and time of reaction.

2.4 FO process and calculations

The process of concentration was conducted in the flowing FO module. The peristaltic pump Jebao auto dosing pump was

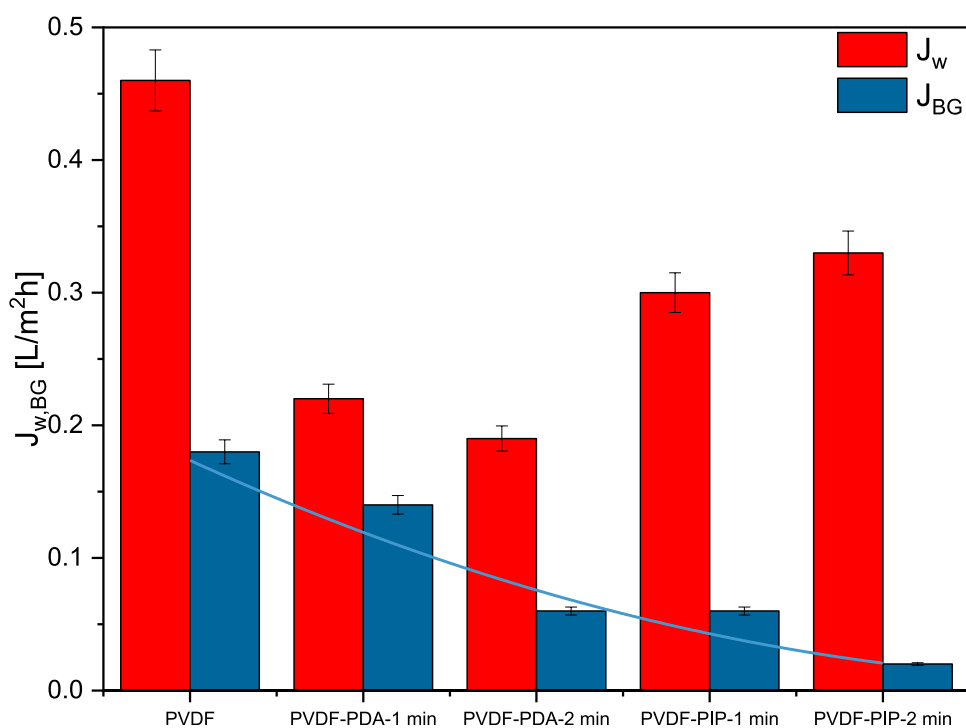


FIGURE 6 Intrinsic separation properties of TFC PVDF membranes: water flux and BG flux for investigated membranes.

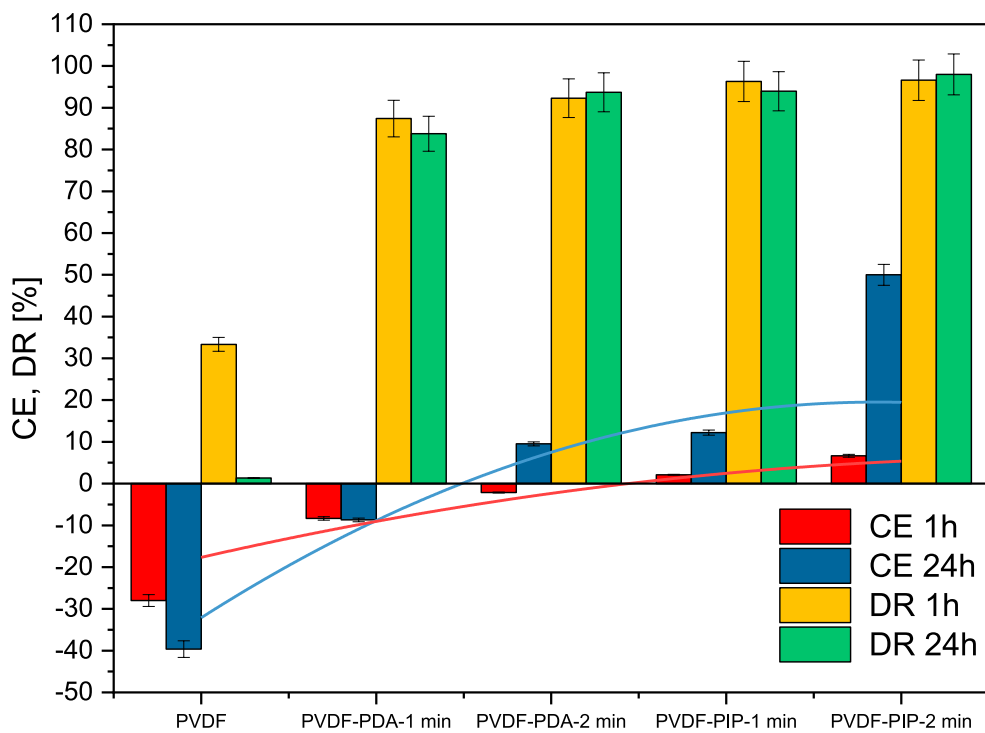


FIGURE 7 Concentration efficiency (CE) and dye rejection (DR) for investigated membrane at various time of FO process.

TABLE 2 FO performance benchmarks of TFC PVDF membranes with different modification paths.

Support	Active layer	Type of compound	Compound flux	Water flux	Ref.
			g/m ² h	L/m ² h	
PVDF/PAN	TMC + MPDA	NaCl	1.9	32.7	Ndiaye et al. (2022)
PVDF	TMC + MPDA	NaCl	8	33	Kallem et al. (2021)
PVDF/PAN	TMC + MPDA	NaCl	3.5	25	Park et al. (2018)
PVDF/GO/MWCNTs	TMC + MPDA	NaCl	1.1	0.34	Yu et al. (2020)
CA/PVDF	TMC + MPDA	NaCl	1.8	32	Shibuya et al. (2018)
PVDF	TMC + MPDA + PEI	MgCl ₂	0.03	1.27	Liu et al. (2017)
PVDF/PFSA	TMC + MPDA	NaCl	7.5	51	Zhang et al. (2017)
PVDF	TMC + MPDA	NaCl	2.33	3.15	Tian et al. (2013)
PVDF/Nylon 6,6	TMC + MPDA	NaCl	27	50	Huang et al. (2016)
PVDF/bentonite	TMC + MPDA	NaCl	5.22	40.64	Shah et al. (2020)
PVDF/SiO ₂ /MWCNTs	TMC + MPDA	NaCl	9	30	Zhang et al. (2018)
PVDF/PDA-PEI	TMC + MPDA	malachite green + NaCl	0.60	29.98	Hu et al. (2021)
PVDF/PMMA + PA-GQD	TMSCI + MDA	Methylene blue, Congo red, NaCl, Mg(NO ₃) ₂	-	170.00	Maiti et al. (2020)
PANI@PAN/PVDF	TMC + MPDA	acid red GR + NaCl	-	40.10	Zhou et al. (2023)
PVD	TMC + DA-PEI	Tannic acid + taurine	0.055	42.10	Li et al. (2022)
PVDF	TMC + MPDA-2min	Glucose	0.6	1.9	This work
PVDF	TMC + PIP-2min	Glucose	0.2	3.3	This work

employed for continuous move of draw and feed solutions with flow rate of 6L/h. As a draw solution, the 10% wt. glucose was applied, while the feed solution was 1% wt. of bromocresol green. The FO process was conducted according to AI-FS strategy, where the active site of prepared membranes is attached to the feed solution. The crucial parameters belonging to the FO are water flux (1), bromocresol green (BG) flux (2), and concentration efficiency (CE). They are given by the following equations:

$$J_w = \frac{\Delta V}{A_m \cdot t} \left[\frac{L}{m^2 \cdot h} \right] \quad (1)$$

$$J_{BG} = \frac{\Delta V_{BG}}{A_m \cdot t} \left[\frac{L}{m^2 \cdot h} \right], \quad (2)$$

$$CE = \frac{C_{BG}(t)}{C_{BG}(0)} \quad (3)$$

$$DR = \left(1 - \frac{C_{BG,drawn}}{C_{BG,feed}} \right) \cdot 100\% \quad (4)$$

ΔV —volume of water [cm³].

ΔV_{BG} —volume of BG [cm³].

A_m —active area of membranes, 13.5 cm².

t —time [h].

C_{BG} —concentration of BG in particular time [g/L].

2.5 Material analysis

2.5.1 Optical microscopy

A TECHREBAL stereo optical microscope was employed for microscopic analysis of the membrane surface. Images of the active layer were captured using the built-in camera within the device.

2.5.2 Fourier transform infrared spectroscopy (FTIR)

Fourier transform infrared spectroscopy (FTIR) in the 4000–400 cm⁻¹ range was carried out using a Jasco 4700 spectrometer equipped with a horizontal attenuated total reflection (ATR) device to identify the functional groups in polymer films. Each analysis involved the accumulation of 64 scans.

2.5.3 Analytical section

Water uptake $W_{H_2O} \left[\frac{g_{H_2O}}{g} \right]$ was calculated according Eq. 5:

$$W_{H_2O} = \frac{(m_{wet} - m_{dry})}{m_{dry}} \quad (5)$$

where m_w is the weight of swollen membrane and m_d is the weight of the dry membrane.

Nitrogen content (Z_N) was determined by Kjeldahl's method after mineralization of the sample (about 200 mg) in concentrated sulphuric acid with copper and potassium sulfates (Table 1).

Grafting yields (G_y) was determined as a balance ration between dry membranes and those after modification, also in dry state. The G_y is express as follows:

$$G_y = \frac{m_{\text{modif,dry}} - m_{\text{umodif,dry}}}{m_{\text{umodif,dry}}} \cdot 100\% \quad (6)$$

Water contact angle (WCA) of the PVDF before modification has been taken by using The Krüss Drop Shape Analyser DS4 (Krüss GmbH, Hamburg, Germany) against distilled water (surface tension 72.0 mN m⁻¹). Following modification, the samples were maintained in a moist state to maintain the activity of functional groups. As a consequence, the WCA was not measured. The complete submersion of the samples in water demonstrates that the membranes are superhydrophilic.

3 Results and discussions

3.1 Physical and chemical characterization of membranes

The physical structure of membranes PVDF are presented at Figure 2. It could be noticed that after modification, the layer of polymerized TMC with MPDA or PIP are visible.

To confirm modification of PVDF nanofibers, the FTIR measurements were performed. The results are presented in Figure 3. The region exhibiting a peak at 875 cm⁻¹ represents the characteristic region for C-H bonds. Similarly, the region at 1015 cm⁻¹ corresponds to C-F bonds. Hence, those peaks confirm the presence of PVDF polymer (Casciola et al., 2005; Pereira et al., 2018).

According to the reactions between TMC with MPDA and PIP, the following specific groups should be found: NH (associated with the aromatic rings), -CNHO (amide groups), -C=O (ketone groups), and -COOH (carboxylic groups). The region displaying a peak at 726 cm⁻¹ is indicative of N-H bonds. At 875 cm⁻¹, the peak is attributed to C-H bonds. The region with a peak at 1015 cm⁻¹ corresponds to C-O bonds, at 1168 cm⁻¹ to C-N amino groups, at 1246 cm⁻¹ to it R-COOH carboxyl groups. Furthermore, at a wavelength of 1401 cm⁻¹, the peak is associated with carbons in C-C aromatics while at region of 1650 cm⁻¹ with the amide groups (Sizeland et al., 2018; Ji et al., 2020). Finally, the region at 1713 cm⁻¹ attributes to ketone bond, C=O. Hence, the presented spectra confirm the reactions between the TMC and PDA, and between TMC and PIP, respectively. Figure 4 depicted the reaction between TMC with PIP and TMC with MPA.

The final parameters describing the performance of obtained membranes are water uptake and grafting yield (G_y). Initially, G_y reflects the effectiveness of modification and the accumulation of polyamide groups on the surface of pristine PVDF. Based on the obtained data, it should be noted t modification efficiency exceeded 10% in all cases. The highest G_y was observed for the reaction of TMC and MPDA for 2 min. Additionally, for PIP modification, a prolonged reaction time resulted in the highest G_y .

The next aspect to be considered is water uptake, a parameter intricately linked to the porosity of PVDF nanofibers. While incorporation of polyamide groups, along with their associated amine groups, may influence water uptake to some extent, the overall change is not so significant. The most notable change occurred for PVDF-PDA-2 min, resulting in a 3.3% increase in water uptake. This observation is directly attributed to the hydrophilic nature of MPDA and PIP, as depicted in Figure 5 (Yang, 2020).

The WCA of the pristine PVDF composite nanofiber membrane was measured to be 90.40° ± 3.40°, indicating that it is hydrophobic. PVDF nanofibers typically exhibit higher hydrophobicity since fluoropolymers usually exhibit low surface energy (Liao et al., 2013; Sethupathy et al., 2013; Rafael et al., 2022). The composite hydrophilicity was altered as a result of the utilisation of copolyamide adhesives.

The final parameter associated with the analysis of the membranes is nitrogen content. The amount of nitrogen is directly linked to the chemical reaction between TMC and aromatic amines. After a 1-min modification in both cases, the Zn levels ranged from 0.13 to 0.19 mmol/g. Increasing the modification time to 2 min resulted in significantly higher Zn value. The successful modification of PVDF is confirmed by the nitrogen content in all investigated cases.

3.2 Forward osmosis investigations

3.2.1 Transport of water and dye by membranes

Water flux and salt rejection factors serve as the most valuable tools for characterizing the properties of TFC membranes. Figure 6 illustrates the impact of various amines and reaction times between them and TMC. It can be observed that water permeability decreased from 0.46 L/m²h for virgin PVDF to 0.19 L/m²h for PVDF-PIP-2min, while dye flux decreased from 0.18 L/m²h for virgin PVDF to 0.02 L/m²h for PVDF-PIP-2min.

Comparing the different types of amines, the nitrogen linked to the cyclic aromatic ring result in a denser layer, as seen in the case of PDA. This phenomenon is evident in the tendency for lower dye fluxes in PVDF-PIP compared to PVDF-PDA. Additionally, the water flux exhibits significantly higher values, with an increase of over 36% and 74% for PVDF-PIP-1min and PVDF-PIP-2min, respectively. The separation properties of the ultrathin polyamide film synthesized via interfacial polymerization are greatly affected by polymerization conditions, including the type of aromatic amines and reaction times. Variations in water flux can be attributed to the differences in structure, morphology, surface properties, and chemistry observed between membranes based on PDA and those based on PIP. Although membranes based on PDA may have reduced water flux as a result of their denser selective layer, membranes based on PIP generally exhibit enhanced water permeability owing to their porous structure.

3.2.2 Concentration of dye by investigated membranes

The forward osmosis performance of TFC PVDF membranes was investigated for its potential to concentrate bromocresol green (BG) dye in the feed solution. The results are presented in Figure 7. In the case of virgin PVDF, it is evident that there was no noticeable

concentration effect of BG. During the FO process, the solution became diluted due to the mixing of liquids. The dye rejection was observed only at the beginning of the process, while the effect disappeared later on. Such phenomenon was expected due to the high porosity of the PVDF nanofibers. In the case of TFC membranes, the dye rejection increased significantly from 33% for PVDF nanofibers to up to 96.6% for PVDF-PIP-2min. However, in the case of PVDF-MPDA-1min, the effect of concentrating BG was not observed. The system prevented BG penetration through the membranes; however, it was unable to extract water. By increasing the reaction time of TMC and MPDA one observed a concentration efficiency of 9.5%.

Replacing the cyclic amines from MPDA to PIP resulted in achieving a dye rejection (DR) of over 90% in all PVDF-PIP cases. The most significant differences were observed in the concentration efficiency (50% for PVDF-PIP-2min membrane. Additionally, dye rejection reached the value of at 98% for this membrane.

4 Comparison to other membranes

The modified PVDF-MPDA and PVDF-PIP membranes are compared with other lab-scale nanofiber PVDF FO membranes. As shown in Table 2, our TFC membrane exhibited comparable water flux and specific salt flux to other nanofiber-based TFC membranes. Interestingly, the modified PVDF-MPDA and PVDF-PIP membranes exhibited the lowest dye flux in the majority of comparable systems. Only PVDF modified by PEI also exhibited a low dye flux of 0.03 g/m²h. With increasing water flux, the salt and other compound flux also rise. This is a general tendency observed for TFC FO membranes. Here, the water flux is limited to only 3.3 L/m²h; however, this system can effectively block BG with a back flux of 0.2 g/m²h.

5 Conclusion

This study investigates the feasibility of using surface-modified hydrophobic PVDF nanofibers as the support for preparation of TFC-FO membrane. In this work, polyamide thin films were synthesized by a reaction between TMC and MPDA and PIP. The type of aromatic amines and time of reaction between them and TMC have a significantly impact on the modification paths and their FO performances. The modification reactions were confirmed by the visibility of characteristic groups at FTIR analysis. The chemical analysis confirmed the presence of nitrogen and grafting yields. The PVDF-PIP-2min exhibited excellent FO performance with water flux at 3.3 LMH and bromocresole green dye rejection at 97% with the possibility to 50% concentrate this dye after 24 h of operation.

References

- Achilli, A., Cath, T. Y., Marchand, E. A., and Childress, A. E. (2009). The forward osmosis membrane bioreactor: a low fouling alternative to MBR processes. *Desalination* 239, 10–21. doi:10.1016/J.DESAL.2008.02.022
- Alihemati, Z., Hashemifard, S. A., Matsuura, T., Ismail, A. F., and Hilal, N. (2020). Current status and challenges of fabricating thin film composite forward osmosis membrane: a comprehensive roadmap. *Desalination* 491, 114557. doi:10.1016/J.DESAL.2020.114557

Data availability statement

The raw data supporting the conclusions of this article will be made available by the authors, without undue reservation. The raw data will be made available upon request.

Author contributions

MM: Writing—original draft, Data curation, Investigation. FY: Investigation, Resources, Writing—original draft, Writing—review and editing. MB: Writing—original draft, Writing—review and editing. AS: Conceptualization, Formal Analysis, Methodology, Supervision, Visualization, Writing—original draft, Writing—review and editing.

Funding

The author(s) declare that financial support was received for the research, authorship, and/or publication of this article. AS supported by the Polish Ministry of Education and Science by the program for outstanding young scientists.

Acknowledgments

AS would like to thank the Department of Process Engineering and Technology of Polymeric and Carbon Materials, Wrocław University of Science and Technology, for financial support from the ministerial subsidy.

Conflict of interest

The authors declare that the research was conducted in the absence of any commercial or financial relationships that could be construed as a potential conflict of interest.

The author(s) declared that they were an editorial board member of *Frontiers*, at the time of submission. This had no impact on the peer review process and the final decision.

Publisher's note

All claims expressed in this article are solely those of the authors and do not necessarily represent those of their affiliated organizations, or those of the publisher, the editors and the reviewers. Any product that may be evaluated in this article, or claim that may be made by its manufacturer, is not guaranteed or endorsed by the publisher.

- Gul, A., Hruza, J., Dvorak, L., and Yalcinkaya, F. (2022). Chemical cleaning process of polymeric nanofibrous membranes. *Polymers* 14, 1102–1114. doi:10.3390/POLYM14061102
- Havelka, O., Yalcinkaya, F., Wacławek, S., Padil, V. V. T., Amendola, V., Černík, M., et al. (2023). Sustainable and scalable development of PVDF-OH Ag/TiO_x nanocomposites for simultaneous oil/water separation and pollutant degradation. *Environ. Sci. Nano* 10, 2359–2373. doi:10.1039/D3EN00335C
- Hu, Y. N., Li, Q. M., Guo, Y. F., Zhu, L. J., Zeng, Z. X., and Xiong, Z. (2021). Nanofiltration-like forward osmosis membranes on *in-situ* mussel-modified polyvinylidene fluoride porous substrate for efficient salt/dye separation. *J. Polym. Sci.* 59, 1065–1071. doi:10.1002/POL.20210138
- Huang, L., Arena, J. T., and McCutcheon, J. R. (2016). Surface modified PVDF nanofiber supported thin film composite membranes for forward osmosis. *J. Memb. Sci.* 499, 352–360. doi:10.1016/J.MEMSCI.2015.10.030
- Huang, L., and McCutcheon, J. R. (2015). Impact of support layer pore size on performance of thin film composite membranes for forward osmosis. *J. Memb. Sci.* 483, 25–33. doi:10.1016/J.MEMSCI.2015.01.025
- Islam, M. N., Yıldırım, B., Maryska, J., and Yalcinkaya, F. (2022). Multi-layered nanofiber membranes: preparation, characterization, and application in wastewater treatment. *J. Industrial Text.* 52, 152808372211274. doi:10.1177/15280837221127443
- Ji, Y., Yang, X., Ji, Z., Zhu, L., Ma, N., Chen, D., et al. (2020). DFT-calculated IR spectrum amide I, II, and III band contributions of N-methylacetamide fine components. *ACS Omega* 5, 8572–8578. doi:10.1021/acsomega.9b04421
- Kallem, P., Gaur, R., Pandey, R. P., Hasan, S. W., Choi, H., and Banat, F. (2021). Thin film composite forward osmosis membranes based on thermally treated PAN hydrophilized PVDF electrospun nanofiber substrates for improved performance. *J. Environ. Chem. Eng.* 9, 106240. doi:10.1016/J.JECE.2021.106240
- Li, K., Li, M., Zhang, W., Xue, Y., Wang, Z., and Zhang, X. (2023). A staged forward osmosis process for simultaneous desalination and concentration of textile wastewaters. *ACS ES T Water* 3, 1817–1825. doi:10.1021/acsestwater.2c00314
- Li, M., Yang, Y., Zhu, L., Wang, G., Zeng, Z., and Xue, L. (2022). Anti-fouling and highly permeable thin-film composite forward osmosis membranes based on the reactive polyvinylidene fluoride porous substrates. *Colloids Surf. A Physicochem Eng. Asp.* 654, 130144. doi:10.1016/J.COLSURFA.2022.130144
- Liao, Y., Wang, R., Tian, M., Qiu, C., and Fane, A. G. (2013). Fabrication of polyvinylidene fluoride (PVDF) nanofiber membranes by electro-spinning for direct contact membrane distillation. *J. Memb. Sci.* 425–426, 30–39. doi:10.1016/J.MEMSCI.2012.09.023
- Lin, C. S., Tung, K. L., Lin, Y. L., Di Dong, C., Chen, C. W., and Wu, C. H. (2020). Fabrication and modification of forward osmosis membranes by using graphene oxide for dye rejection and sludge concentration. *Process Saf. Environ. Prot.* 144, 225–235. doi:10.1016/J.PSEP.2020.07.007
- Liu, C., Lei, X., Wang, L., Jia, J., Liang, X., Zhao, X., et al. (2017). Investigation on the removal performances of heavy metal ions with the layer-by-layer assembled forward osmosis membranes. *Chem. Eng. J.* 327, 60–70. doi:10.1016/J.CEJ.2017.06.070
- Maiti, S., Samantaray, P. K., and Bose, S. (2020). *In situ* assembly of a graphene oxide quantum dot-based thin-film nanocomposite supported on de-mixed blends for desalination through forward osmosis. *Nanoscale Adv.* 2, 1993–2003. doi:10.1039/C9NA00688E
- Ndiaye, I., Chaoui, I., Eddouibi, J., Vaudreuil, S., and Bounahmidi, T. (2022). Synthesis of poly (vinylidene fluoride)/polyacrylonitrile electrospun substrate-based thin-film composite membranes for desalination by forward osmosis process. *Chem. Eng. Process. - Process Intensif.* 181, 109132. doi:10.1016/J.CEP.2022.109132
- Park, M. J., Gonzales, R. R., Abdel-Wahab, A., Phuntsho, S., and Shon, H. K. (2018). Hydrophilic polyvinyl alcohol coating on hydrophobic electrospun nanofiber membrane for high performance thin film composite forward osmosis membrane. *Desalination* 426, 50–59. doi:10.1016/J.DESAL.2017.10.042
- Peng, L. E., Yao, Z., Chen, J., Guo, H., and Tang, C. Y. (2020). Highly selective separation and resource recovery using forward osmosis membrane assembled by polyphenol network. *J. Memb. Sci.* 611, 118305. doi:10.1016/J.MEMSCI.2020.118305
- Pereira, E. L. M., Batista, A. de S. M., Alves, N., de Oliveira, A. H., Ribeiro, F. A. S., Santos, A. P., et al. (2018). Effects of the addition of MWCNT and ZrO₂ nanoparticles on the dosimetric properties of PVDF. *Appl. Radiat. Isotopes* 141, 275–281. doi:10.1016/J.APRADISO.2018.07.015
- Qiu, G., and Ting, Y. P. (2013). Osmotic membrane bioreactor for wastewater treatment and the effect of salt accumulation on system performance and microbial community dynamics. *Bioresour. Technol.* 150, 287–297. doi:10.1016/J.BIORTECH.2013.09.090
- Rafael, R., Rosas, R., Rosas, J. M., García-Mateos, F. J., Pisarenko, T., Papež, N., et al. (2022). Comprehensive characterization of PVDF nanofibers at macro- and nanolevel. *Polymers* 14, 593. doi:10.3390/POLYM14030593
- Sethupathy, M., Sethuraman, V., Manisankar, P., Sethupathy, M., Sethuraman, V., and Manisankar, P. (2013). Preparation of PVDF/SiO₂ and PVDF/PAA/SiO₂ Composite Nanofiber Membrane Using Electrospinning for Polymer Electrolyte Analysis. *Soft Nanosci. Lett.* 3, 37–43. doi:10.4236/SNL.2013.32007
- Shah, A. A., Cho, Y. H., Nam, S. E., Park, A., Park, Y. I., and Park, H. (2020). High performance thin-film nanocomposite forward osmosis membrane based on PVDF/bentonite nanofiber support. *J. Industrial Eng. Chem.* 86, 90–99. doi:10.1016/J.JIEC.2020.02.016
- Shibuya, M., Park, M. J., Lim, S., Phuntsho, S., Matsuyama, H., and Shon, H. K. (2018). Novel CA/PVDF nanofiber supports strategically designed via coaxial electrospinning for high performance thin-film composite forward osmosis membranes for desalination. *Desalination* 445, 63–74. doi:10.1016/J.DESAL.2018.07.025
- Sizeland, K. H., Hofman, K. A., Hallett, I. C., Martin, D. E., Potgieter, J., Kirby, N. M., et al. (2018). Nanostructure of electrospun collagen: do electrospun collagen fibers form native structures? *Mater. (Oxf)* 3, 90–96. doi:10.1016/J.MTLA.2018.10.001
- Tian, M., Qiu, C., Liao, Y., Chou, S., and Wang, R. (2013). Preparation of polyamide thin film composite forward osmosis membranes using electrospun polyvinylidene fluoride (PVDF) nanofibers as substrates. *Sep. Purif. Technol.* 118, 727–736. doi:10.1016/J.SEPPUR.2013.08.021
- Torres-Mendieta, R., Yalcinkaya, F., Boyraz, E., Havelka, O., Wacławek, S., Maryska, J., et al. (2020). PVDF nanofibrous membranes modified via laser-synthesized Ag nanoparticles for a cleaner oily water separation. *Appl. Surf. Sci.* 526, 146575. doi:10.1016/J.APSUSC.2020.146575
- Xiao, D., Tang, C. Y., Zhang, J., Lay, W. C. L., Wang, R., and Fane, A. G. (2011). Modeling salt accumulation in osmotic membrane bioreactors: implications for FO membrane selection and system operation. *J. Memb. Sci.* 366, 314–324. doi:10.1016/J.MEMSCI.2010.10.023
- Yalcinkaya, F., Siekierka, A., and Bryjak, M. (2017). Surface modification of electrospun nanofibrous membranes for oily wastewater separation. *RSC Adv.* 7, 56704–56712. doi:10.1039/C7RA11904F
- Yang, X. (2020). Monitoring the interfacial polymerization of piperazine and trimesoyl chloride with hydrophilic interlayer or macromolecular additive by *in situ* FT-IR spectroscopy. *Membranes* 10, 12–10. doi:10.3390/MEMBRANES10010012
- Yu, F., Shi, H., Shi, J., Teng, K., Xu, Z., and Qian, X. (2020). High-performance forward osmosis membrane with ultra-fast water transport channel and ultra-thin polyamide layer. *J. Memb. Sci.* 616, 118611. doi:10.1016/J.MEMSCI.2020.118611
- Zhang, X., Shen, L., Guan, C. Y., Liu, C. X., Lang, W. Z., and Wang, Y. (2018). Construction of SiO₂@MWNTs incorporated PVDF substrate for reducing internal concentration polarization in forward osmosis. *J. Memb. Sci.* 564, 328–341. doi:10.1016/J.MEMSCI.2018.07.043
- Zhang, X., Shen, L., Lang, W. Z., and Wang, Y. (2017). Improved performance of thin-film composite membrane with PVDF/PFSA substrate for forward osmosis process. *J. Memb. Sci.* 535, 188–199. doi:10.1016/J.MEMSCI.2017.04.038
- Zhao, P., Gao, B., Xu, S., Kong, J., Ma, D., Shon, H. K., et al. (2015). Polyelectrolyte-promoted forward osmosis process for dye wastewater treatment – exploring the feasibility of using polyacrylamide as draw solute. *Chem. Eng. J.* 264, 32–38. doi:10.1016/J.CEJ.2014.11.064
- Zhou, L., Yu, H., Yamin Hossain, M., Chen, F., Du, C., and Zhang, G. (2023). Fabrication of high-performance forward osmosis membrane based on asymmetric integrated nanofiber porous support induced by a new controlled photothermal induction method. *Chem. Eng. J.* 470, 144366. doi:10.1016/J.CEJ.2023.144366